

Tri- and Tetra-superatomic Molecules in Ligand-Protected Face-Fused Icosahedral (M@Au₁₂)_n (M = Au, Pt, Ir, and Os, and n = 3 and 4) Clusters

Chang Xu,[†] Yichun Zhou,[†] Jiuqi Yi, Dan Li, Lili Shi, and Longjiu Cheng*



Cite This: *J. Phys. Chem. Lett.* 2022, 13, 1931–1939



Read Online

ACCESS |



Metrics & More

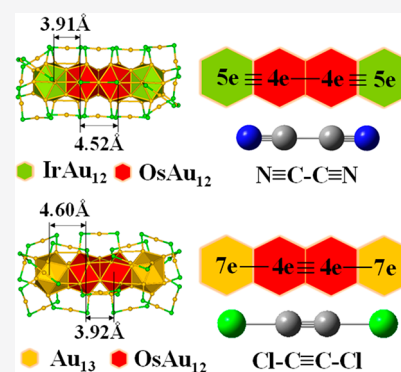


Article Recommendations



Supporting Information

ABSTRACT: Cluster assembling has been one of the hottest topics in nanochemistry. In certain ligand-protected gold clusters, bi-icosahedral cores assembled from Au₁₃ superatoms were found to be analogues of diatomic molecules F₂, N₂, and singlet O₂, respectively, in electronic shells, depending upon the super valence bond (SVB) model. However, challenges still remain for extending the scale in cluster assembling via the SVB model. In this work, ligand-protected tri- and tetra-superatomic clusters composed of icosahedral M@Au₁₂ (M = Au, Pt, Ir, and Os) units are theoretically predicted. These clusters are stable with reasonable highest occupied molecular orbital (HOMO)–lowest unoccupied molecular orbital (LUMO) energy gaps and proven to be analogues of simple triatomic (Cl₃[−], OCl₂, O₃, and CO₂) and tetra-atomic (N≡C–C≡N, and Cl–C≡C–Cl) molecules in both geometric and electronic structures. Moreover, a stable cluster-assembling gold nanowire is predicted following the same rules. This work provides effective electronic rules for cluster assembling on a larger scale and gives references for their experimental synthesis.



Ligand-protected gold clusters have been intensively studied during the past decades as a result of their intriguing properties and wide potential applications.^{1–12} Certain gold clusters are described as superatoms (SAs), because electron shell configurations of their Au cores follow the Jellium model, in which valence electrons fill discrete superatomic orbitals (1s²1p⁶1d¹⁰2s²1f¹⁴...).^{13–17} Stabilities for a number of Au_m(SR)_n clusters are confirmed by the superatom model, such as Au₁₂(SR)₉⁺, Au₂₅(SR)₁₈[−], Au₄₄(SR)₂₈^{2−}, Au₆₈(SR)₃₄, and Au₁₀₂(SR)₄₄, which have 2e, 8e, 18e, 34e, and 58e Au cores, respectively.^{18–23} Among them, the closed-packed Au₁₃ core of Au₂₅(SR)₁₈[−] is the structure frequently observed in gold nanostructures^{24–28} as a result of its magic character associated with 8e electronic closed-shell (1s²1p⁶) and icosahedral geometry. The central atom in icosahedral Au₁₃ can be replaced by other metal atoms to regulate the number of their valence electrons,^{29–35} and these icosahedrons are rational building blocks for cluster assembling.^{36–44}

A number of assemblies composed of all-gold icosahedrons or monometallic-doped icosahedrons have been obtained, in which the icosahedral units are linked through ligands, interatomic bonds, or van der Waals interactions conventionally.^{42–50} The super valence bond (SVB) model proposed by our group^{51–53} gives the new perspective for the electronic shell of superatomic clusters, which points out that superatoms can form superatomic molecules through the SVB by sharing nuclei and valence electrons. On the basis of the SVB model,

the bi-icosahedral cores in [Au₂₀(PPhy₂)₁₀Cl₄]Cl₂,⁵² Au₃₈(SR)₂₄,^{53,54} Au₂₂(dppo)₆,⁵⁵ and Au₂₂H₄(dppo)₆⁵⁶ clusters are proven to be bi-superatomic molecules with super single, triple, and quadruple bonds through density functional theory (DFT) calculations, which can be considered as analogues of diatomic molecules, such as F₂, N₂, and Re₂, in electron shells. The electronic structure of the Au₂Ag₄₂ core in Au₂Ag₄₂(SAdm)₂₇(BPh₄) clusters is reported as dimerization of two 8e superatoms, similar to Ne₂.⁵⁷ Beside the linear structure, SVBs are also observed in some three-dimensional arrays, including [Au₆{Ni₃(CO)₆}₄]^{2−} and Au₇₀S₂₀(PPh₃)₁₂, reported by Muñoz-Castro.^{58,59} Moreover, a series of clusters formed by two icosahedral M@Au₁₂ (M = Pd and Pt) superatoms are theoretically designed on the basis of the SVB model and targetedly synthesized by Tsukuda et al.,⁶⁰ of which one has an electronic configuration similar to that of singlet O₂. The bond orders of SVBs in M₂Au₃₆(SR)₂₄ (M = Au, Pd, and Pt) clusters can be reversibly controlled by tuning their charge states, to obtain the single-, double-, and triple-bonded superatomic molecules.⁶¹

Received: January 3, 2022

Accepted: February 17, 2022

Table 1. Symmetries, HOMO–LUMO Energy Gaps (E_{H-L}), Lengths of SVBs (R_{SA-SA}), Number of Valence Electrons for Tri- and Tetra-superatomic Molecules Formed by $M@Au_{12}$ ($M = Au, Pt, Ir, \text{ and } Os$) Icosahedrons, and Their Analogues (PBE0/def2svp)

superatomic molecule	symmetry	E_{H-L} (eV)	R_{SA-SA} (Å) ^a	valence electrons	analogue
$[Au_{33}(Au_{18}Cl_{30})]^-$ (1)	S_6	1.39	4.16	22e	Cl_3^-
$[PtAu_{32}(Au_{18}Cl_{30})]$ (2)	S_6	1.55	4.23	20e	OCl_2
$[OsPt_2Au_{30}(Au_{18}Cl_{30})]$ (3)	S_6	0.70	4.30	16e	CO_2
$[Pt_3Au_{30}(Au_{18}Cl_{30})]$ (4)	S_6	1.19	4.22	18e	O_3
$[Os_2Ir_2Au_{39}(Au_{21}Cl_{36})]$ (5)	D_3	1.05	4.52 (3.91) ^b	18e	$N\equiv C-C\equiv N$
$[Os_2Au_{41}(Au_{21}Cl_{36})]$ (6)	D_3	1.30	3.92 (4.60) ^c	22e	$Cl-C\equiv C-Cl$

^a R_{SA-SA} is defined as distances between central metals in adjacent superatomic icosahedrons. ^b R_{Os-Os} (R_{Os-Ir}). ^c R_{Os-Os} (R_{Os-Au}).

The SVB model reveals the bonding rule between two homogeneous superatoms, which provide another possible pattern for cluster assembly, that is, assembling superatoms in the same way as atoms. Thus far, a number of bi-superatomic molecules are designed following the SVB model, but further development is still needed to reveal the possibility for superatom assembling on a larger scale based on the same rule.

In this paper, efforts are made to extend the superatomic framework to tri- and tetra-superatomic molecules through the SVB model. The ligand-protected tri- and tetra-icosahedron clusters formed by face-sharing $M@Au_{12}$ ($M = Au, Pt, Ir, \text{ and } Os$) superatomic icosahedrons are designed. In each $M@Au_{12}$ icosahedral superatom, 12 Au atoms on the surface are either protected by staple motifs or shared with other superatoms, and thus, each atom contributes 0.5 valence electrons to the superatomic shell (6e in total). Because different atomic dopants provide different numbers of valence electrons in the Jellium potential, the series of metal-doped [$M = Au, Pt, Ir, \text{ and } Os$] superatoms can be treated as electronic analogues of Cl, O, N, and C atoms with seven, six, five, and four valence electrons, respectively. Therefore, these tri- and tetra-superatomic molecules are proven to be electronic analogues of Cl_3^- , OCl_2 , CO_2 , O_3 , $N\equiv C-C\equiv N$, and $Cl-C\equiv C-Cl$ molecules in their bonding frameworks. Following the same rule, a stable superatomic nanowire composed of $Pt@Au_{12}$ icosahedrons is predicted, as a linear assembling of 6e superatoms, in which the electronic shell closure is obtained through super valence bonds.

Here, geometric structures of these superatom assemblies are built and fully optimized at the PBE0⁶²/def2svp⁶³ level of theory. All structures are verified to be true minima by frequency check. A halogen (Cl) is chosen to replace thioalcohol ligands, which are commonly used in experiments to simplify the geometric structure, and it is confirmed that the electronic shell of $Au_{25}Cl_{18}$ is almost identical to that of $Au_{25}(SR)_{18}$.⁶⁴ The formulas of these cluster are written as [core(ligand)]^{ion} for convenience. As shown in Table 1, these clusters have similar geometric symmetries and fairly large highest occupied molecular orbital (HOMO)–lowest unoccupied molecular orbital (LUMO) gaps.

The geometry of $[Au_{33}(Au_{18}Cl_{30})]^-$ (1) is formed by face-fused tri-icosahedral Au_{13} cores, as shown in Figure 1a, of which 24 vertexes are stapled by six Au_2Cl_3 and six $AuCl_2$ oligomers (Figure 1b). It could be viewed as a union of three Au_{13} icosahedrons, in which a Au_3 triangle face is shared by the two adjacent icosahedral units (Figure 1c).

The electronic shell of the Au_{33} core in $[Au_{33}(Au_{18}Cl_{30})]^-$ (1) is further discussed. Because each staple motif withdraws one electron, the Au_{33} core with a tri-icosahedral structure has 22 valence electrons, which is supposed to be an analogue of

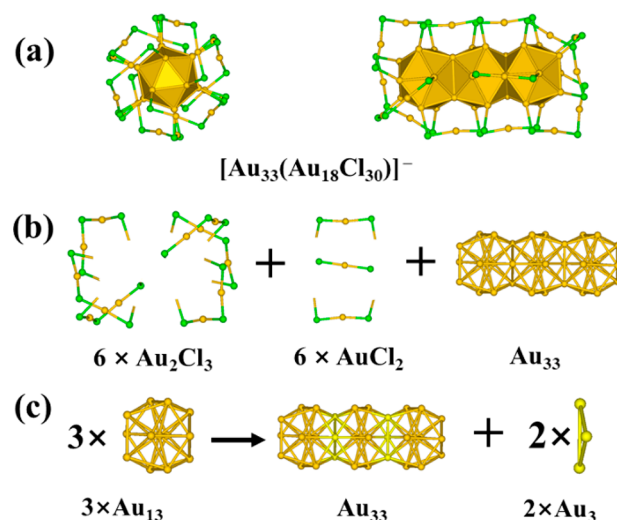


Figure 1. (a) Top and side views of tri-superatomic molecule $[Au_{33}(Au_{18}Cl_{30})]^-$ (1). The Au_2Cl_3 and $AuCl_2$ staple motifs are given in ball-and-stick pattern, and the Au cores are shown as polyhedrons. (b) Assembling of the Au_{33} core, Au_2Cl_3 , and $AuCl_2$ staple motifs. (c) Formation of the prolate Au_{33} core from Au_{13} superatoms (Au, yellow; Cl, green).

the Cl_3^- molecule in both electronic and geometric structures. To verify our inference, the bonding pattern of Au_{33} is investigated using the adaptive natural density partition (AdNDP) method,⁶⁵ which is widely used in discussions of localized multicenter chemical bonding. The results reveal that this Au_{33} core is formed by three open-shell SAs through SVBs. As shown in Figure 2a, there are three 13c–2e super lone pairs (LPs) (super s, p_x, and p_y) in each SA. The p_z orbitals in three SAs compose one σ bonding, one $n\sigma$ non-bonding, and one σ^* anti-bonding orbitals, and the former two orbitals are occupied as three superatomic center–two electron (3sc–2e) super bonds. As we know, in the Cl_3^- molecule, there are three LPs in each atom and two 3c–2e σ bonds (one s and one n σ), as shown in Figure 2b. Therefore, this Au_{33} core is an electronically analogous to Cl_3^- in the bonding framework. Moreover, a comparison of the Kohn–Sham molecular orbitals (MOs) between the $[Au_{33}(Au_{18}Cl_{30})]^-$ cluster and Cl_3^- molecule also confirms their similarity in electronic shells (Figure S1 of the Supporting Information). This superatom bonding pattern is different from the $[Au_{37}(PPh_3)_{10}(SR)_{10}X_2]^+$ cluster, which was theoretically predicted in 2007 and experimentally obtained in 2015.^{42,66} The Au_{37} core in $[Au_{37}(PPh_3)_{10}(SR)_{10}X_2]^+$ also shows a rod-like structure composed of three icosahedral Au_{13} units, but it is assembled through vertex–vertex fusion rather than the face–face pattern.

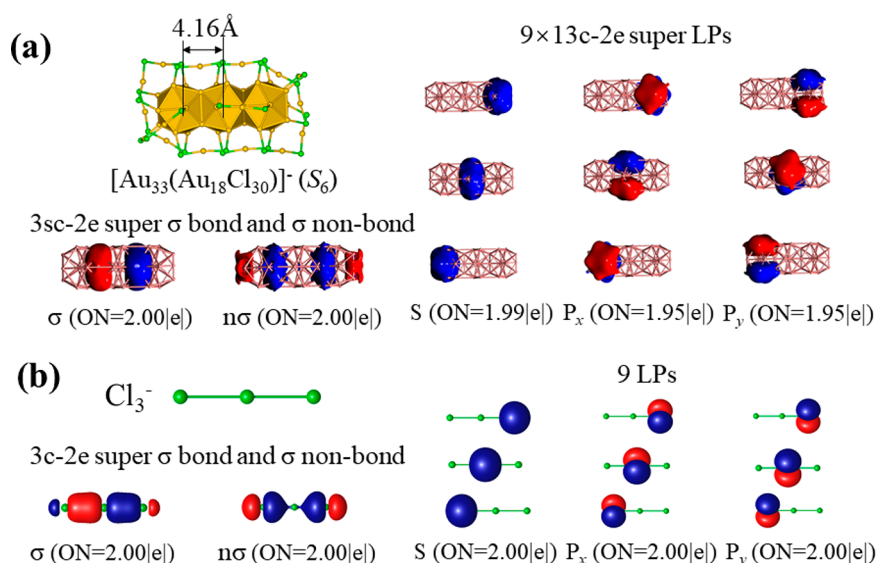


Figure 2. Structures, AdNDP localized bonds, and electronic occupation numbers (ONs) of the (a) Au_{33} core in tri-superatomic molecule $[\text{Au}_{33}(\text{Au}_{18}\text{Cl}_{30})]^-$ (1) and (b) Cl_3^- molecule.

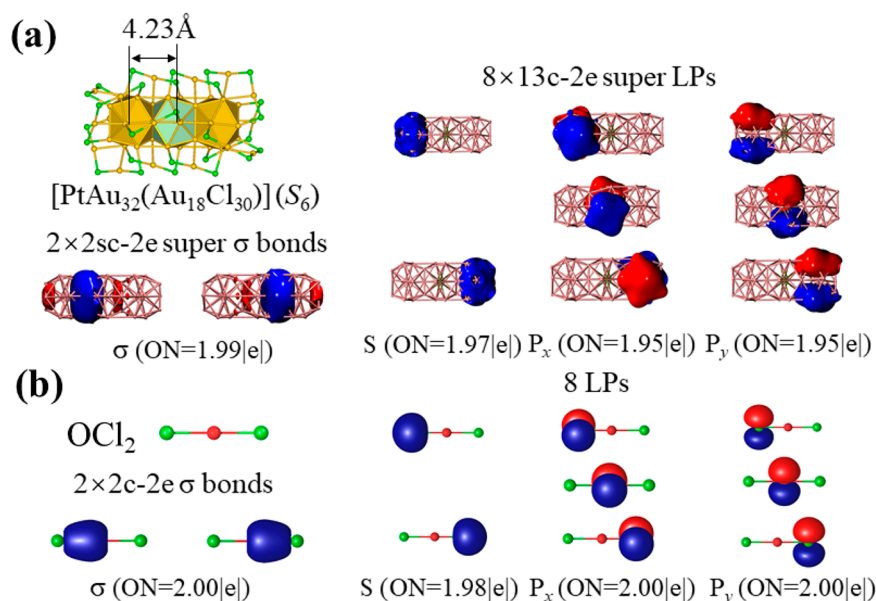


Figure 3. Structures, AdNDP localized bonds, and electronic ONs of the (a) PtAu_{32} core in tri-superatomic molecule $[\text{PtAu}_{32}(\text{Au}_{18}\text{Cl}_{30})]$ (2) and (b) OCl_2 molecule (Au₁₃, yellow polyhedron; Pt@Au₁₂, green polyhedron).

As shown in Figure S2 of the Supporting Information, each icosahedral Au_{13} is a closed-shell SA ($1s^21p^6$), and they form a stable tri-superatom molecule through the superatom networks⁶⁷ without sharing valence electrons.

The PtAu_{32} core in $[\text{PtAu}_{32}(\text{Au}_{18}\text{Cl}_{30})]$ (2) is also formed by three face-sharing icosahedra, but it has 20 valence electrons, which is two electrons less than the core in $[\text{Au}_{33}(\text{Au}_{18}\text{Cl}_{30})]^-$ (1), and could be taken into comparison with the linear OCl_2 molecule. The tri-superatomic electronic shell of this PtAu_{32} core is confirmed by AdNDP results in Figure 3a. There are three 13c-2e super LPs (super s, p_x , and p_y) in each SA on the sides and two LPs (super p_x and p_y) in the middle SA. Two 2sc-2e super σ bonds are formed by sp hybrid orbitals of the middle SA and the p_z orbital of two side SAs, to reach the electronic shell closure. It is actually an electronic analogue of the OCl_2 molecule with two 2c-2e σ bonds formed by sp

hybrid orbitals of the O atom and the p_z orbital of the Cl atom (Figure 3b).

The $\text{OsPt}_2\text{Au}_{30}$ core in $[\text{OsPt}_2\text{Au}_{30}(\text{Au}_{18}\text{Cl}_{30})]$ (3) has a geometry similar to that of the Au_{33} core composed of three face-fused icosahedra, but the Au atoms in centers of three Au_{13} cages are replaced by one Os (middle) and two Pt (sides) atoms, respectively, to change the number of valence electrons. This $\text{OsPt}_2\text{Au}_{30}$ core with 16 valence electrons is also supposed to be a tri-superatomic molecule. The AdNDP calculation reveals that there is one super LP (super s) in each $\text{Pt}@Au_{12}$ icosahedron, and the rest of the 12 valence electrons occupy two 2sc-2e super σ bonds, two 3sc-2e super π bonds, and two $n\pi$ bonds. Dependent upon the orbital shape, two super σ bonds are formed by the sp hybrid orbitals of $\text{Os}@Au_{12}$ and the p_z orbitals in $\text{Pt}@Au_{12}$, respectively, and other four super $\pi/n\pi$ bonds are formed by $p_x-p_x-p_x$ and $p_y-p_y-p_y$

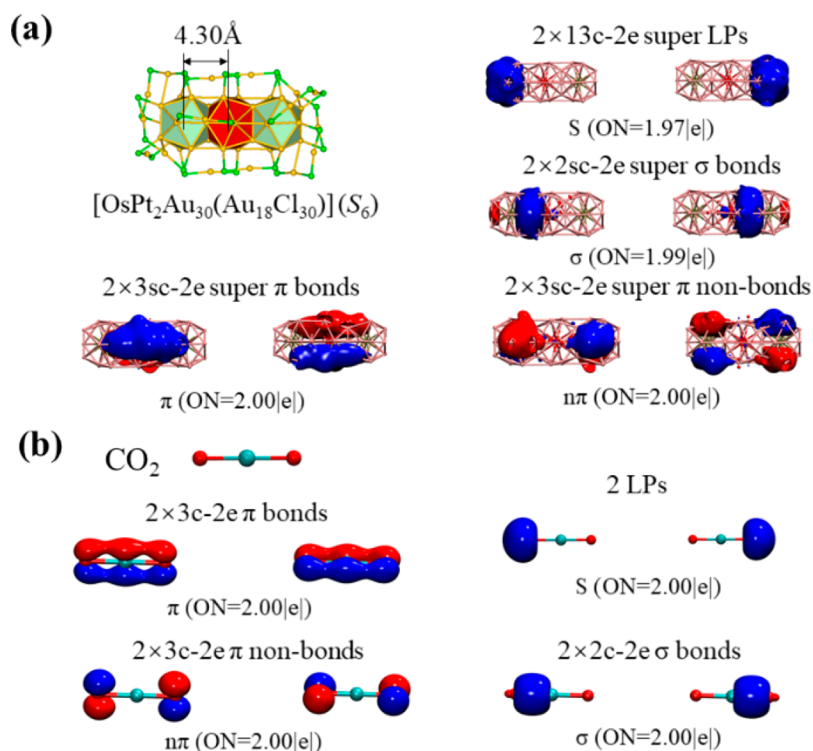


Figure 4. Structures, AdNDP localized bonds, and electronic ONs of the (a) $\text{OsPt}_2\text{Au}_{30}$ core in tri-superatomic molecule $[\text{OsPt}_2\text{Au}_{30}(\text{Au}_{18}\text{Cl}_{30})]$ (3) and (b) CO_2 molecule (Pt@Au₁₂, green polyhedron; Os@Au₁₂, red polyhedron).

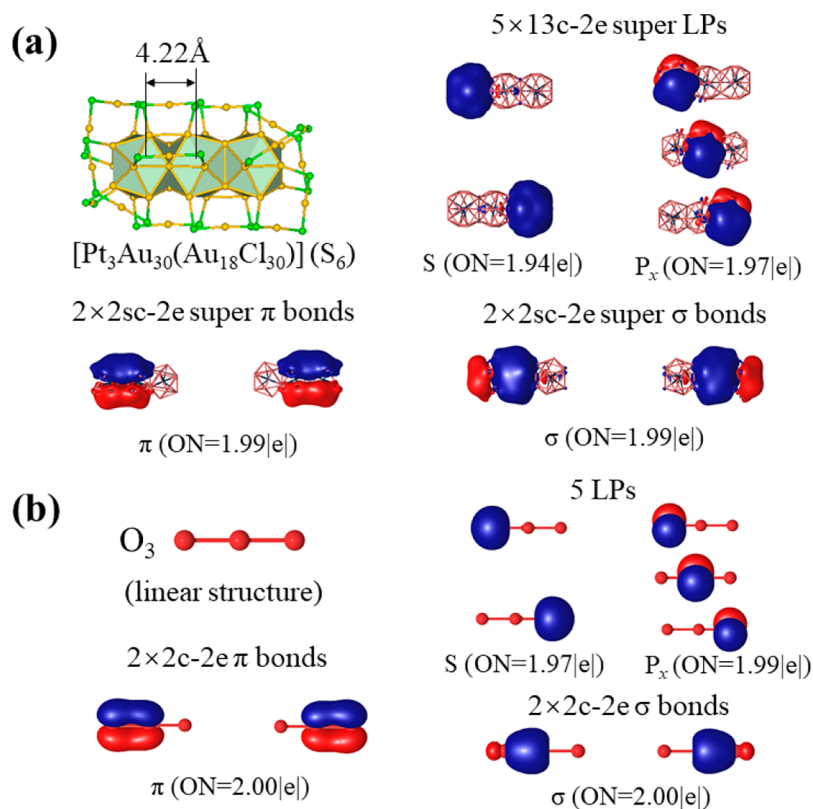


Figure 5. Structures, AdNDP localized bonds, and electronic ONs of the (a) $\text{Pt}_3\text{Au}_{30}$ core in tri-superatomic molecule $[\text{Pt}_3\text{Au}_{30}(\text{Au}_{18}\text{Cl}_{30})]$ (4) and (b) linear O_3 molecule.

interactions between three icosahedrons. Therefore, the $\text{OsPt}_2\text{Au}_{30}$ core is composed of one 4e open-shell superatom (Os@Au₁₂ with $1s^21p^2$) and two 6e open-shell superatoms

(Pt@Au₁₂ with $1s^21p^4$) through two super double bonds. The molecule-like electronic shell closure of $\text{OsPt}_2\text{Au}_{30}$ is an analogue of the CO_2 molecule (Figure 4b).

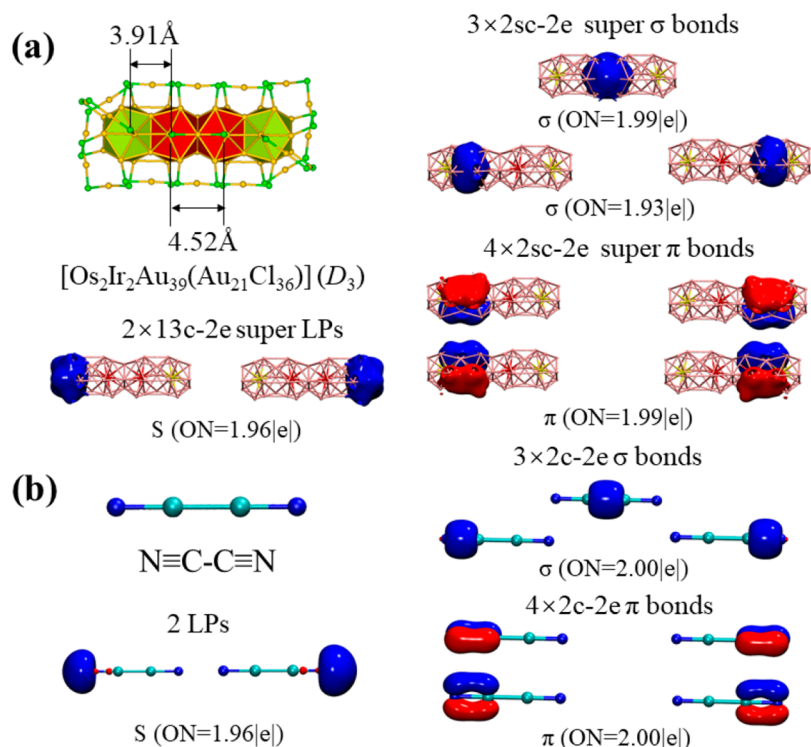


Figure 6. Structures, AdNDP localized bonds, and electronic ONs of the (a) $Os_2Ir_2Au_{39}$ core in tetra-superatomic molecule $[Os_2Ir_2Au_{39}(Au_{21}Cl_{36})]$ (5) and (b) $N \equiv C-C \equiv N$ molecule ($Ir@Au_{12}$, green polyhedron; $Os@Au_{12}$, red polyhedron).

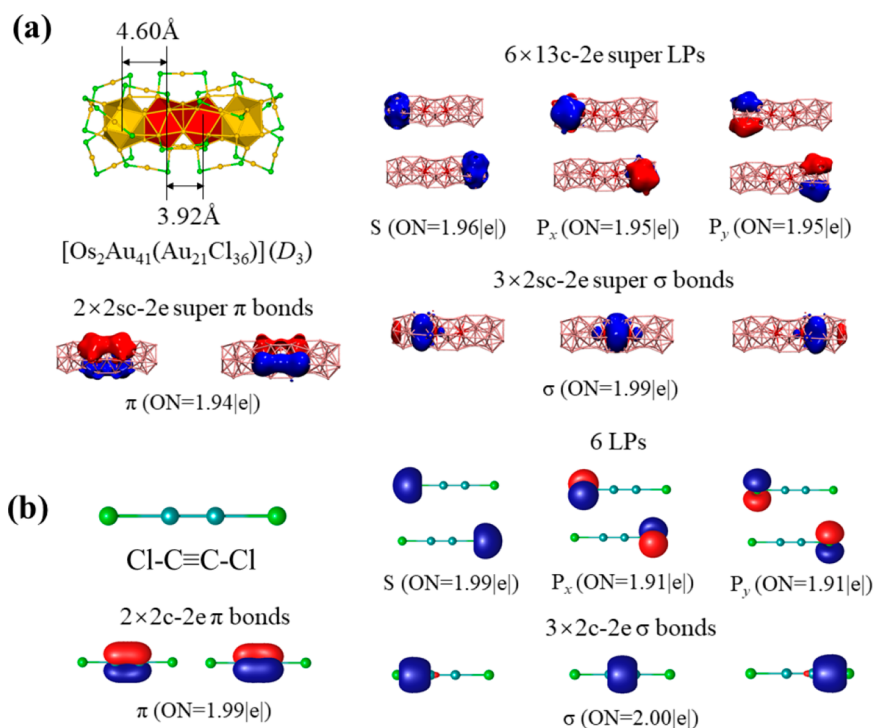


Figure 7. Structures, AdNDP localized bonds, and electronic ONs of the (a) Os_2Au_{41} core in tetra-superatomic molecule $[Os_2Au_{41}(Au_{21}Cl_{36})]$ cluster (6) and (b) $Cl-C \equiv C-Cl$ molecule (Au_{13} , yellow polyhedron; $Os@Au_{12}$, red polyhedron).

Then, we use the Pt atom to replace the Os atom in the center of $[OsPt_2Au_{30}(Au_{18}Cl_{30})]$ (3), to obtain a superatomic analogue of the linear O_3 molecule. The Pt_3Au_{30} core of the $[Pt_3Au_{30}(Au_{18}Cl_{30})]$ (4) cluster has 18 electrons, in which each $Pt@Au_{12}$ icosahedron has 6 valence electrons and could be viewed as open-shell SAs ($1s^21p^4$) depending upon the

AdNDP analysis. As shown in Figure 5a, there are two $13c-2e$ super LPs (super s and p_x) in each $Pt@Au_{12}$ SA on the side and one $13c-2e$ super LP (super p_x) in central $Pt@Au_{12}$ SA. The molecule-like electronic shell closure of Pt_3Au_{30} is achieved through two $2sc-2e$ super σ bonds and two $2sc-2e$ super π bonds, similar to that of the linear O_3 molecule.

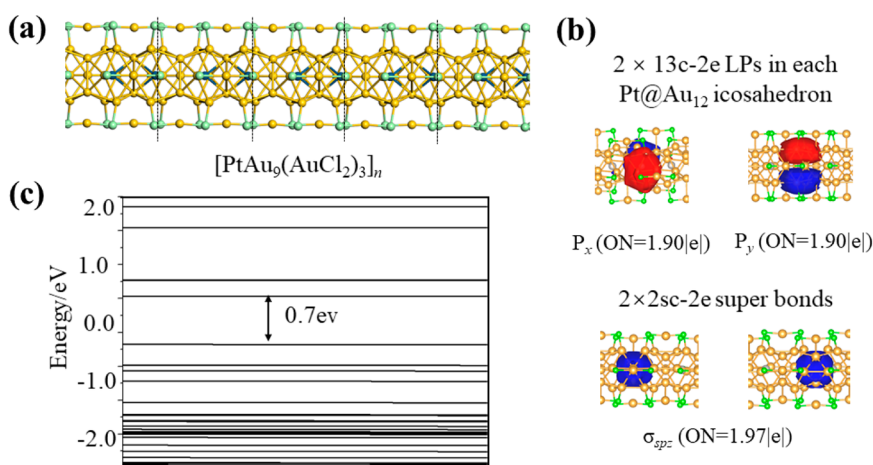


Figure 8. (a) Geometry of ligand-protected face-sharing $[\text{PtAu}_9(\text{AuCl}_2)_3]_n$ nanowires, (b) AdNDP localized bonds and ONs of three icosahedral Pt@Au_{12} units in a $2 \times 1 \times 1$ supercell (PBE/def2svp), and (c) electronic band structure of $[\text{PtAu}_9(\text{AuCl}_2)_3]_n$ (PBE) (Au, yellow; Pt, gray; and Cl, green).

However, as we know, the global minimum structure of O_3 is V-shaped, as the atomic orbitals in the central O atom undergo sp^2 hybridization.

The tetra-superatomic molecules are predicted in the same way. The $\text{Os}_2\text{Ir}_2\text{Au}_{39}$ core of linear $[\text{Os}_2\text{Ir}_2\text{Au}_{39}(\text{Au}_{21}\text{Cl}_{36})]_n$ (5) is formed by four face-sharing $M@Au_{12}$ ($M = \text{Os}$ and Ir ; Os in the middle and Ir on the sides) icosahedrons. There are 18 valence electrons in this tetra-icosahedral core, and the lengths between adjacent icosahedral cages are different (4.52 Å between two Os atoms and 3.91 Å between adjacent Ir and Os atoms); thus, it is supposed to be a tetra-superatomic molecule similar to $\text{N}\equiv\text{C}-\text{C}\equiv\text{N}$ with interval single and triple bonds. AdNDP analysis confirms this inference. As shown in Figure 6a, there is one $13\text{c}-2\text{e}$ super LP (super s) in each Ir@Au_{12} SA, and the seven $2\text{sc}-2\text{e}$ super bonds consisted of three σ -bonding orbitals formed by p_z (in each Ir@Au_{12} SA) and sp hybrid orbitals (in each Os@Au_{12} SA) and four double-degenerate π bonds composed of p_x-p_x and p_y-p_y interactions (in Ir@Au_{12} and Os@Au_{12} SAs). Therefore, there is one single bond and two super triple bonds in the $\text{Os}_2\text{Ir}_2\text{Au}_{39}$ core, which is in accordance with the electronic shell of the $\text{N}\equiv\text{C}-\text{C}\equiv\text{N}$ molecule, as shown in Figure 6b.

The $\text{Os}_2\text{Au}_{41}$ core of the $[\text{Os}_2\text{Au}_{41}(\text{Au}_{21}\text{Cl}_{36})]_n$ cluster (6) has a geometric structure similar to that of $\text{Ir}_2\text{Os}_2\text{Au}_{39}$, but the electronic shells are different because two Ir atoms in $\text{Ir}_2\text{Os}_2\text{Au}_{39}$ are substituted by two Au atoms. The lengths between two Os atoms and adjacent Au and Os atoms are 3.92 and 4.60 Å, respectively; thus, we suppose that the electronic shell of $\text{Os}_2\text{Au}_{41}$ would be similar to that of the $\text{Cl}-\text{C}\equiv\text{C}-\text{Cl}$ molecule. AdNDP results in Figure 7a reveal that there are three $13\text{c}-2\text{e}$ super LPs (super s, p_x , and p_y) localized in each Au_{13} icosahedron, three $2\text{sc}-2\text{e}$ super σ bonds formed by p_z (in each Au_{13} SA) and sp hybrid orbitals (in each Os@Au_{12} SA), and two $2\text{sc}-2\text{e}$ π bonds composed of double-degenerate π bonds of p_x-p_x and p_y-p_y (in each Os@Au_{12} SA). Therefore, there is one super triple bond and two super single bonds in the $\text{Os}_2\text{Au}_{41}$ core, and the superatomic bonding framework ($3\sigma 2\pi$) is a nice analogue of the $\text{Cl}-\text{C}\equiv\text{C}-\text{Cl}$ molecule.

Lengths of the super bonds also present important evidence for the superatomic bonding characters in these tetra-superatomic molecules. All of the superatomic molecules are composed of the icosahedral $M@Au_{12}$ cage, and the super

bond length is defined as the distance between central metals in adjacent superatoms (as shown in Table 1). For $[\text{Os}_2\text{Ir}_2\text{Au}_{39}(\text{Au}_{21}\text{Cl}_{36})]_n$, the super single bond length ($R_{\text{Os}-\text{Os}} = 4.52$ Å) is obviously larger than the super triple bond ($R_{\text{Ir}-\text{Os}} = 3.91$ Å), which is in accordance with its bonding characters. The super bond lengths in $[\text{Os}_2\text{Au}_{41}(\text{Au}_{21}\text{Cl}_{36})]_n$ also confirm its bonding pattern, in which the super single bond ($R_{\text{Au}-\text{Os}} = 4.60$ Å) is longer than the super triple bond ($R_{\text{Os}-\text{Os}} = 3.92$ Å). Moreover, in their electronic shells, more electrons are localized within the super triple bonds between superatoms, resulting in higher electronic density, where can be a potential reactive site for electrophilic reagents.^{7,41}

Finally, we extend the superatomic framework to one-dimensional nanowires following the same bonding rule. Figure 8a shows the optimized geometry of the $[\text{PtAu}_9(\text{AuCl}_2)_3]_n$ nanowire. The unit cell of this gold nanowire contains two face-sharing Pt@Au_{12} icosahedrons, with the optimized lattice constants of $a = b = 50$ Å and $c = 8.43$ Å. The super bond length between two icosahedral SAs (4.22 Å) in this nanowire is almost the same as a super single bond (4.23 Å) in the $[\text{PtAu}_{32}(\text{Au}_{18}\text{Cl}_{30})]_n$ (2) cluster.

Solid-state adaptive natural density partitioning (SSAdNDP)⁶⁸ analysis is carried out to gain the bonding pattern in the $[\text{PtAu}_9(\text{AuCl}_2)_3]_n$ nanowire. The bonding analysis is performed in three icosahedral SAs with a $2 \times 1 \times 1$ supercell, and the results identify that there are two $13\text{c}-2\text{e}$ super LPs (super p_x and p_y) in each Pt@Au_{12} SA and one $2\text{sc}-2\text{e}$ super σ bonding orbital is formed by sp hybrid orbitals of adjacent SAs to achieve electronic shell closure, as shown in Figure 8b. As expected, this nanowire is a semiconductor with a band gap of 0.7 eV (PBE), because valence electron pairs are localized in either one superatom as super LPs or between two superatoms as super bonds. However, in the pure gold nanowire with similar face-sharing geometry, reported by Whetten et al.,³⁶ there is one more valence electron in each icosahedron, in which the electronic shell closure of the SVB model cannot be satisfied; thus, this nanowire is metallic.

Ab initio molecular dynamics (AIMD) simulations are further performed to confirm the thermal stability of the $[\text{PtAu}_9(\text{AuCl}_2)_3]_n$ nanowire. The unit cell (24 Au atoms, 2 Pt atoms, and 12 Cl atoms) is adopted as the initial configuration. Energy fluctuation depending upon the simulated time at 300 K and the snapshot of Pt@Au_{12} after a 10 ps AIMD simulation

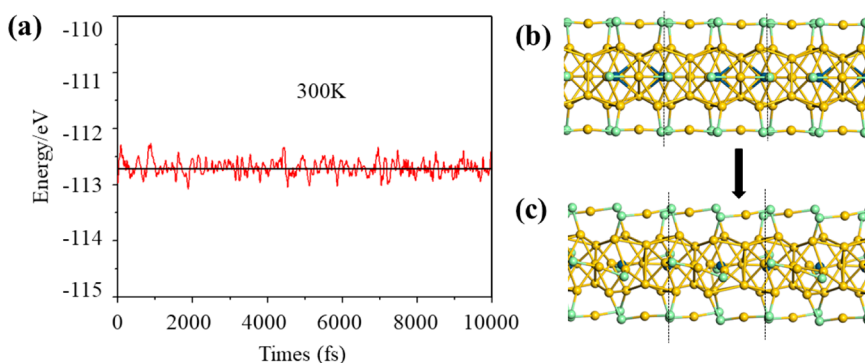


Figure 9. (a) Energy fluctuation depending upon simulated time in molecular dynamics simulation at 300 K and snapshots of (b) initial structure and (c) after a 10 ps AIMD simulation for the $[\text{PtAu}_9(\text{AuCl}_2)_3]_n$ nanowire (Au, yellow; Pt, gray; and Cl, green).

are plotted in panels b and c of Figure 9. It can be observed that the structure of the nanowire maintains integrity with only a slight disturbance of individual atoms during the 10 ps AIMD simulation, indicating its good thermal stability at room temperature.

In conclusion, we extend the SVB model to the possibility of tri- and tetra-superatomic molecules formed by $(\text{M}@\text{Au}_{12})_n$ ($\text{M} = \text{Au}, \text{Pt}, \text{Ir}, \text{and Os}$, and $n = 3$ and 4) icosahedral units. Chemical bonding analysis reveals that the bonding framework of tri-superatomic molecules $[\text{M}_3\text{Au}_{30}(\text{Au}_{18}\text{Cl}_{30})]$ ($\text{M} = \text{Au}, \text{Pt}$, and Os) (1–4) is similar to Cl_3^- , OCl_2 , O_3 , and CO_2 , and the tetra-superatomic molecules $[\text{M}_4\text{Au}_{39}(\text{Au}_{21}\text{Cl}_{36})]$ ($\text{M} = \text{Au}, \text{Ir}$, and Os) (5 and 6) are analogues of $\text{N}\equiv\text{C}-\text{C}\equiv\text{N}$ and $\text{Cl}-\text{C}\equiv\text{C}-\text{Cl}$. The lengths of super triple bonds are shorter than those of super single bonds in these tetra-superatomic molecules, which is another evidence for their superatomic bonding character. Subsequently, the one-dimensional $[\text{PtAu}_9(\text{AuCl}_2)_3]_n$ superatomic nanowire is designed following the same bonding rule, in which each icosahedral $\text{Pt}@\text{Au}_{12}$ SA forms one super σ bond with its adjacent one. The geometric and electronic stability of this nanowire has been confirmed, and the length of its super σ bond is approximate to a single super bond in the $[\text{PtAu}_{32}(\text{Au}_{18}\text{Cl}_{30})]$ (2) cluster. This paper explores electronic rules for cluster assembling from superatoms to multi-superatomic molecules and superatomic nanowires, which gives references for their experimental synthesis.

■ ASSOCIATED CONTENT

Supporting Information

The Supporting Information is available free of charge at <https://pubs.acs.org/doi/10.1021/acs.jpcllett.2c00007>.

Computational details and relative references, comparison of Kohn–Sham molecular orbitals for $[\text{Au}_{33}(\text{Au}_{18}\text{Cl}_{30})]^-$ and Cl_3^- (Figure S1), structures and localized bonds of the Au_{37} core in $[\text{Au}_{37}(\text{PPh}_3)_{10}(\text{SR})_{10}\text{X}_2]^+$ (Figure S2), and Cartesian coordinates of structures 1–6 reported in this work (PDF)

■ AUTHOR INFORMATION

Corresponding Author

Longjiu Cheng – Department of Chemistry and Key Laboratory of Structure and Functional Regulation of Hybrid Materials, Anhui University, Hefei, Anhui 230601, People's

Republic of China; orcid.org/0000-0001-7086-6190;
Email: clj@ustc.edu

Authors

Chang Xu – Department of Chemistry, Anhui University, Hefei, Anhui 230601, People's Republic of China
Yichun Zhou – Department of Chemistry, Anhui University, Hefei, Anhui 230601, People's Republic of China
Jiuqi Yi – Department of Chemistry, Anhui University, Hefei, Anhui 230601, People's Republic of China
Dan Li – Department of Chemistry, Anhui University, Hefei, Anhui 230601, People's Republic of China
Lili Shi – Department of Chemistry, Anhui University, Hefei, Anhui 230601, People's Republic of China; orcid.org/0000-0001-7938-1907

Complete contact information is available at:
<https://pubs.acs.org/10.1021/acs.jpcllett.2c00007>

Author Contributions

[†]Chang Xu and Yichun Zhou contributed equally to this work.

Notes

The authors declare no competing financial interest.

■ ACKNOWLEDGMENTS

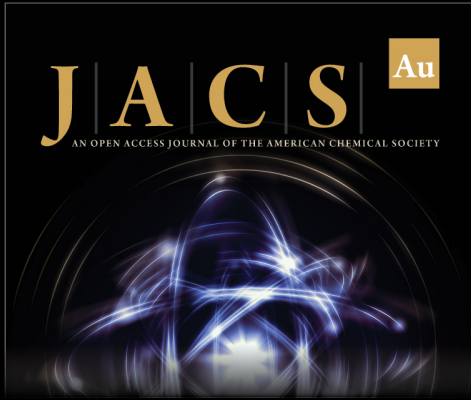
Longjiu Cheng acknowledges support from the National Natural Science Foundation of China (Grant 21873001) and the Foundation of Distinguished Young Scientists of Anhui Province. Chang Xu acknowledges support from the National Natural Science Foundation of China (Grant 22103001), the Natural Science Foundation of Anhui Province (Grant 2108085QB64), and the Natural Science Research Project for Colleges and Universities of Anhui Province (Grant KJ2019A0009). The calculations are carried out at the High-Performance Computing Center of Anhui University.

■ REFERENCES

- (1) Li, G.; Jin, R. C. Atomically Precise Gold Nanoclusters as New Model Catalysts. *Acc. Chem. Res.* **2013**, *46*, 1749–1758.
- (2) Li, G.; Jiang, D. E.; Kumar, S.; Chen, Y. X.; Jin, R. C. Size Dependence of Atomically Precise Gold Nanoclusters in Chemo-selective Hydrogenation and Active Site Structure. *ACS Catal.* **2014**, *4*, 2463–2469.
- (3) Jin, R.; Zeng, C.; Zhou, M.; Chen, Y. Atomically Precise Colloidal Metal Nanoclusters and Nanoparticles: Fundamentals and Opportunities. *Chem. Rev.* **2016**, *116*, 10346–10413.
- (4) Hu, G. X.; Tang, Q.; Lee, D.; Wu, Z. L.; Jiang, D. E. Metallic Hydrogen in Atomically Precise Gold Nanoclusters. *Chem. Mater.* **2017**, *29*, 4840–4847.


- (5) Tang, Q.; Hu, G.; Fung, V.; Jiang, D. E. Insights into Interfaces, Stability, Electronic Properties, and Catalytic Activities of Atomically Precise Metal Nanoclusters from First Principles. *Acc. Chem. Res.* **2018**, *51*, 2793–2802.
- (6) Zhao, J.; Jin, R. Heterogeneous Catalysis by Gold and Gold-Based Bimetal Nanoclusters. *Nano Today* **2018**, *18*, 86–102.
- (7) Higaki, T.; Li, Y.; Zhao, S.; Li, Q.; Li, S.; Du, X. S.; Yang, S.; Chai, J.; Jin, R. Atomically Tailored Gold Nanoclusters for Catalytic Application. *Angew. Chem., Int. Ed. Engl.* **2019**, *58*, 8291–8302.
- (8) Kang, X.; Li, Y. W.; Zhu, M. Z.; Jin, R. C. Atomically Precise Alloy Nanoclusters: Syntheses, Structures, and Properties. *Chem. Soc. Rev.* **2020**, *49*, 6443–6514.
- (9) Du, X. S.; Jin, R. C. Atomic-Precision Engineering of Metal Nanoclusters. *Dalton Trans.* **2020**, *49*, 10701–10707.
- (10) Li, Y.; Zhou, M.; Jin, R. Programmable Metal Nanoclusters with Atomic Precision. *Adv. Mater.* **2021**, *33*, 2006591.
- (11) Jin, R.; Li, G.; Sharma, S.; Li, Y.; Du, X. Toward Active-Site Tailoring in Heterogeneous Catalysis by Atomically Precise Metal Nanoclusters with Crystallographic Structures. *Chem. Rev.* **2021**, *121*, 567–648.
- (12) Cheng, A.; Wang, R.; Liu, Z.; Liu, R.; Huang, W.; Wang, Z. Charge “Skin Behavior” of Gold Superatoms. *J. Phys. Chem. Lett.* **2021**, *12*, 8713–8719.
- (13) Brack, M. The Physics of Simple Metal-Clusters Self-Consistent Jellium Model and Semiclassical Approaches. *Rev. Mod. Phys.* **1993**, *65*, 677–732.
- (14) Deheer, W. A. The Physics of Simple Metal-Clusters—Experimental Aspects and Simple-Models. *Rev. Mod. Phys.* **1993**, *65*, 611–676.
- (15) Luo, Z.; Castleman, A. W. Special and General Superatoms. *Acc. Chem. Res.* **2014**, *47*, 2931–2940.
- (16) Jena, P.; Sun, Q. Super Atomic Clusters: Design Rules and Potential for Building Blocks of Materials. *Chem. Rev.* **2018**, *118*, 5755–5870.
- (17) Takano, S.; Tsukuda, T. Chemically Modified Gold/Silver Superatoms as Artificial Elements at Nanoscale: Design Principles and Synthesis Challenges. *J. Am. Chem. Soc.* **2021**, *143*, 1683–1698.
- (18) Gao, Y. Ligand Effects of Thiolate-Protected Au₁₀₂ Nanoclusters. *J. Phys. Chem. C* **2013**, *117*, 8983–8988.
- (19) Jiang, D. E.; Walter, M.; Akola, J. On the Structure of a Thiolated Gold Cluster: Au₄₄(SR)₂₈²⁻. *J. Phys. Chem. C* **2010**, *114*, 15883–15889.
- (20) Jiang, D. E.; Whetten, R. L.; Luo, W. D.; Dai, S. The Smallest Thiolated Gold Superatom Complexes. *J. Phys. Chem. C* **2009**, *113*, 17291–17295.
- (21) Dass, A. Mass Spectrometric Identification of Au₆₈(SR)₃₄ Molecular Gold Nanoclusters with 34-Electron Shell Closing. *J. Am. Chem. Soc.* **2009**, *131*, 11666–11667.
- (22) Zhu, M.; Aikens, C. M.; Hollander, F. J.; Schatz, G. C.; Jin, R. Correlating the Crystal Structure of a Thiol-Protected Au₂₅ Cluster and Optical Properties. *J. Am. Chem. Soc.* **2008**, *130*, 5883–5885.
- (23) Walter, M.; Akola, J.; Lopez-Acevedo, O.; Jadzinsky, P. D.; Calero, G.; Ackerson, C. J.; Whetten, R. L.; Grönbeck, H.; Häkkinen, H. A Unified View of Ligand-Protected Gold Clusters as Superatom Complexes. *Proc. Natl. Acad. Sci. U. S. A.* **2008**, *105*, 9157–9162.
- (24) Munoz-Castro, A. Potential of N-Heterocyclic Carbene Derivatives from Au₁₃(dppe)₃Cl₂ Gold Superatoms. Evaluation of Electronic, Optical and Chiroptical Properties from Relativistic DFT. *Inorg. Chem. Front.* **2019**, *6*, 2349–2358.
- (25) Fedik, N.; Boldyrev, A. I.; Munoz-Castro, A. Aromatic Character of [Au₁₃]⁵⁺ and [MAu₁₂]^{4+/6+} (M = Pd, Pt) Cores in Ligand Protected Gold Nanoclusters—Interplay between Spherical and Planar σ -Aromatics. *Phys. Chem. Chem. Phys.* **2019**, *21*, 25215–25219.
- (26) Kwak, K.; Choi, W.; Tang, Q.; Jiang, D. E.; Lee, D. Rationally Designed Metal Nanocluster for Electrocatalytic Hydrogen Production from Water. *J. Mater. Chem. A* **2018**, *6*, 19495–19501.
- (27) Matsuo, S.; Yamazoe, S.; Goh, J. Q.; Akola, J.; Tsukuda, T. The Electrooxidation-Induced Structural Changes of Gold Di-Superatomic Molecules: Au₂₃ vs. Au₂₅. *Phys. Chem. Chem. Phys.* **2016**, *18*, 4822–4827.
- (28) Sugiuchi, M.; Shichibu, Y.; Nakanishi, T.; Hasegawa, Y.; Konishi, K. Cluster- π Electronic Interaction in a Superatomic Au₁₃ Cluster Bearing σ -Bonded Acetylide Ligands. *Chem. Commun.* **2015**, *51*, 13519–13522.
- (29) Hossain, S.; Ono, T.; Yoshioka, M.; Hu, G. X.; Hosoi, M.; Chen, Z. H.; Nair, L. V.; Niihori, Y.; Kurashige, W.; Jiang, D. E.; et al. Thiolate-Protected Trimetallic Au_{~20}Ag_{~4}Pd and Au_{~20}Ag_{~4}Pt Alloy Clusters with Controlled Chemical Composition and Metal Positions. *J. Phys. Chem. Lett.* **2018**, *9*, 2590–2594.
- (30) Choi, W.; Hu, G. X.; Kwak, K.; Kim, M.; Jiang, D. E.; Choi, J. P.; Lee, D. Effects of Metal-Doping on Hydrogen Evolution Reaction Catalyzed by MAu₂₄ and M₂Au₃₆ Nanoclusters (M = Pt, Pd). *ACS Appl. Mater. Interfaces* **2018**, *10*, 44645–44653.
- (31) Munoz-Castro, A. Doping the Cage. Re@Au₁₁Pt and Ta@Au₁₁Hg, as Novel 18-ve Trimetallic Superatoms Displaying a Doped Icosahedral Golden Cage. *Phys. Chem. Chem. Phys.* **2017**, *19*, 2459–2465.
- (32) Alkan, F.; Munoz-Castro, A.; Aikens, C. M. Relativistic DFT Investigation of Electronic Structure Effects Arising from Doping the Au₂₅ Nanocluster with Transition Metals. *Nanoscale* **2017**, *9*, 15825–15834.
- (33) Munoz-Castro, A. The Impact of Endohedral Atoms on the Electronic and Optical Properties of Au₂₅(SR)₁₈ and Au₃₈(SR)₂₄. *Phys. Chem. Chem. Phys.* **2016**, *18*, 31419–31423.
- (34) Kwak, K.; Tang, Q.; Kim, M.; Jiang, D. E.; Lee, D. Interconversion between Superatomic 6-Electron and 8-Electron Configurations of M@Au₂₄(SR)₁₈ Clusters (M = Pd, Pt). *J. Am. Chem. Soc.* **2015**, *137*, 10833–10840.
- (35) Jin, R.; Nobusada, K. Doping and Alloying in Atomically Precise Gold Nanoparticles. *Nano Research* **2014**, *7*, 285–300.
- (36) Jiang, D. E.; Nobusada, K.; Luo, W. D.; Whetten, R. L. Thiolated Gold Nanowires: Metallic Versus Semiconducting. *ACS Nano* **2009**, *3*, 2351–2357.
- (37) Song, Y.; Fu, F.; Zhang, J.; Chai, J.; Kang, X.; Li, P.; Li, S.; Zhou, H.; Zhu, M. The Magic Au₆₀ Nanocluster: A New Cluster-Assembled Material with Five Au₁₃ Building Blocks. *Angew. Chem., Int. Ed.* **2015**, *54*, 8430–8434.
- (38) Yamazoe, S.; Takano, S.; Kurashige, W.; Yokoyama, T.; Nitta, K.; Negishi, Y.; Tsukuda, T. Hierarchy of Bond Stiffnesses within Icosahedral-Based Gold Clusters Protected by Thiolates. *Nat. Commun.* **2016**, *7*, 10414.
- (39) Higaki, T.; Li, Q.; Zhou, M.; Zhao, S.; Li, Y.; Li, S.; Jin, R. Toward the Tailoring Chemistry of Metal Nanoclusters for Enhancing Functionalities. *Acc. Chem. Res.* **2018**, *51*, 2764–2773.
- (40) Gam, F.; Liu, C. W.; Kahlal, S.; Saillard, J. Y. Electron Counting and Bonding Patterns in Assemblies of Three and More Silver-Rich Superatoms. *Nanoscale* **2020**, *12*, 20308–20316.
- (41) Li, Y.; Li, S.; Nagarajan, A. V.; Liu, Z.; Nevins, S.; Song, Y.; Mpourmpakis, G.; Jin, R. Hydrogen Evolution Electrocatalyst Design: Turning Inert Gold into Active Catalyst by Atomically Precise Nanochemistry. *J. Am. Chem. Soc.* **2021**, *143*, 11102–11108.
- (42) Jin, R. X.; Liu, C.; Zhao, S.; Das, A.; Xing, H. Z.; Gayathri, C.; Xing, Y.; Rosi, N. L.; Gil, R. R.; Jin, R. C. Tri-Icosahedral Gold Nanocluster [Au₃₇(PPh₃)₁₀(SC₂H₄Ph)₁₀X₂]⁺: Linear Assembly of Icosahedral Building Blocks. *ACS Nano* **2015**, *9*, 8530–8536.
- (43) Kang, X.; Zhu, M. Intra-Cluster Growth Meets Inter-Cluster Assembly: The Molecular and Supramolecular Chemistry of Atomically Precise Nanoclusters. *Coord. Chem. Rev.* **2019**, *394*, 1–38.
- (44) Yuan, P.; Zhang, R.; Selenius, E.; Ruan, P.; Yao, Y.; Zhou, Y.; Malola, S.; Häkkinen, H.; Teo, B. K.; Cao, Y.; Zheng, N. Solvent-Mediated Assembly of Atom-Precise Gold–Silver Nanoclusters to Semiconducting One-Dimensional Materials. *Nat. Commun.* **2020**, *11*, 2229.
- (45) De Nardi, M.; Antonello, S.; Jiang, D.-e.; Pan, F.; Rissanen, K.; Ruzzi, M.; Venzo, A.; Zoleo, A.; Maran, F. Gold Nanowired: A Linear (Au₂₅)_n Polymer from Au₂₅ Molecular Clusters. *ACS Nano* **2014**, *8*, 8505–8512.


- (46) Chen, J.; Zhang, Q. F.; Bonaccorso, T. A.; Williard, P. G.; Wang, L. S. Controlling Gold Nanoclusters by Diphosphine Ligands. *J. Am. Chem. Soc.* **2014**, *136*, 92–95.
- (47) Liu, L.; Yuan, J.; Cheng, L.; Yang, J. New Insights into the Stability and Structural Evolution of Some Gold Nanoclusters. *Nanoscale* **2017**, *9*, 856–861.
- (48) Chakraborty, P.; Nag, A.; Chakraborty, A.; Pradeep, T. Approaching Materials with Atomic Precision Using Supramolecular Cluster Assemblies. *Acc. Chem. Res.* **2019**, *52*, 2–11.
- (49) Du, X.; Chai, J.; Yang, S.; Li, Y.; Higaki, T.; Li, S.; Jin, R. Fusion Growth Patterns in Atomically Precise Metal Nanoclusters. *Nanoscale* **2019**, *11*, 19158–19165.
- (50) Tian, Z.; Xu, Y.; Cheng, L. New Perspectives on the Electronic and Geometric Structure of Au₇₀S₂₀(PPh₃)₁₂ Cluster: Superatomic-Network Core Protected by Novel Au₁₂(μ₃-S)₁₀ Staple Motifs. *Nanomaterials* **2019**, *9*, 1132.
- (51) Cheng, L. J.; Yang, J. L. Communication: New Insight into Electronic Shells of Metal Clusters: Analogues of Simple Molecules. *J. Chem. Phys.* **2013**, *138*, 141101.
- (52) Yuan, Y.; Cheng, L.; Yang, J. Electronic Stability of Phosphine-Protected Au₂₀ Nanocluster: Superatomic Bonding. *J. Phys. Chem. C* **2013**, *117*, 13276–13282.
- (53) Cheng, L. J.; Ren, C. D.; Zhang, X. Z.; Yang, J. L. New Insight into the Electronic Shell of Au₃₈(SR)₂₄: A Superatomic Molecule. *Nanoscale* **2013**, *5*, 1475–1478.
- (54) Liu, Q.; Xu, C.; Wu, X.; Cheng, L. Electronic Shells of a Tubular Au₂₆ Cluster: A Cage–Cage Superatomic Molecule Based on Spherical Aromaticity. *Nanoscale* **2019**, *11*, 13227–13232.
- (55) Munoz-Castro, A. Triple 1D≡1D Superatomic Bonding. Au₂₂(dppo)₆ as a Π⁴- and Δ²-Triply Bonded Cluster Based on Au₁₁ Assembled Units. *Phys. Chem. Chem. Phys.* **2020**, *22*, 1422–1426.
- (56) Dong, J.; Gao, Z. H.; Zhang, Q. F.; Wang, L. S. The Synthesis, Bonding, and Transformation of a Ligand-Protected Gold Nanohydride Cluster. *Angew. Chem., Int. Ed.* **2021**, *60*, 2424–2430.
- (57) Jin, S.; Zou, X. J.; Xiong, L.; Du, W. J.; Wang, S. X.; Pei, Y.; Zhu, M. Z. Bonding of Two 8-Electron Superatom Clusters. *Angew. Chem., Int. Ed.* **2018**, *57*, 16768–16772.
- (58) Muñoz-Castro, A. Au₇₀S₂₀(PPh₃)₁₂ as Superatomic Analog to 18-Electron Transition-Metal Complexes. *Z. Anorg. Allg. Chem.* **2021**, *647*, 1819–1823.
- (59) Muñoz-Castro, A. sp³-Hybridization in Superatomic Clusters. Analogues to Simple Molecules Involving the Au₆ Core. *Chem. Sci.* **2014**, *5*, 4749–4754.
- (60) Ito, E.; Takano, S.; Nakamura, T.; Tsukuda, T. Controlled Dimerization and Bonding Scheme of Icosahedral M@Au₁₂ (M = Pd, Pt) Superatoms. *Angew. Chem., Int. Ed. Engl.* **2021**, *60*, 645–649.
- (61) Munoz-Castro, A. Single, Double, and Triple Intercluster Bonds: Analyses of M₂Au₃₆(SR)₂₄ (M = Au, Pd, Pt) as 14-, 12- and 10-ve Superatomic Molecules. *Chem. Commun. (Camb)* **2019**, *55*, 7307–7310.
- (62) Adamo, C.; Barone, V. Toward Reliable Density Functional Methods without Adjustable Parameters: The PBE0 Model. *J. Chem. Phys.* **1999**, *110*, 6158–6170.
- (63) Weigend, F.; Ahlrichs, R. Balanced Basis Sets of Split Valence, Triple Zeta Valence and Quadruple Zeta Valence Quality for H to Rn: Design and Assessment of Accuracy. *Phys. Chem. Chem. Phys.* **2005**, *7*, 3297–3305.
- (64) Tian, Z.; Cheng, L. Perspectives on the Energy Landscape of Au–Cl Binary Systems from the Structural Phase Diagram of Au_xCl_y (x + y = 20). *Phys. Chem. Chem. Phys.* **2015**, *17*, 13421–13428.
- (65) Zubarev, D. Y.; Boldyrev, A. I. Developing Paradigms of Chemical Bonding: Adaptive Natural Density Partitioning. *Phys. Chem. Chem. Phys.* **2008**, *10*, 5207–5217.
- (66) Shichibu, Y.; Negishi, Y.; Watanabe, T.; Chaki, N. K.; Kawaguchi, H.; Tsukuda, T. Biicosahedral Gold Clusters [Au₂₅(PPh₃)₁₀(SC_nH_{2n+1})₅Cl₂]²⁺ (n = 2–18): A Stepping Stone to Cluster-Assembled Materials. *J. Phys. Chem. C* **2007**, *111*, 7845–7847.
- (67) Cheng, L. J.; Yuan, Y.; Zhang, X. Z.; Yang, J. L. Superatom Networks in Thiolate-Protected Gold Nanoparticles. *Angew. Chem., Int. Ed.* **2013**, *52*, 9035–9039.
- (68) Galeev, T. R.; Dunnington, B. D.; Schmidt, J. R.; Boldyrev, A. I. Solid State Adaptive Natural Density Partitioning: A Tool for Deciphering Multi-Center Bonding in Periodic Systems. *Phys. Chem. Chem. Phys.* **2013**, *15*, 5022–5029.



JACS Au
AN OPEN ACCESS JOURNAL OF THE AMERICAN CHEMICAL SOCIETY

Editor-in-Chief
Prof. Christopher W. Jones
Georgia Institute of Technology, USA

Open for Submissions 

pubs.acs.org/jacsau  ACS Publications
Most Trusted. Most Cited. Most Read.